Damage nucleation and vacancy-induced structural transformation in Si grain boundaries

A. Maiti[a] and S. T. Pantelides
Solid State Division, Oak Ridge National Laboratory, Oak Ridge, Tennessee 37831
and Department of Physics and Astronomy, Vanderbilt University, Nashville, Tennessee 37235

M. F. Chisholm and S. J. Pennycook
Solid State Division, Oak Ridge National Laboratory, Oak Ridge, Tennessee 37831

(Received 13 February 1999; accepted for publication 16 August 1999)

Atomic resolution *Z*-contrast scanning transmission electron microscopy reveals preferential nucleation of electron-beam-induced damage in select atomic columns of a Si tilt grain boundary. Atomic scale simulations find that the region of initial damage nucleation corresponds to columns where the formation energies of vacancies and vacancy complexes are very low. The calculations further predict that vacancy accumulation in certain pairs of columns can induce a structural transformation to low-density dislocation ''pipes'' with all atoms fourfold coordinated. © *1999 American Institute of Physics.* [S0003-6951(99)00742-1]

Beam-induced processing is a widely studied phenomenon,[1] and it has long been known that beam-induced amorphization nucleates preferentially at extended defects such as grain boundaries.[2] The electron microscope has also been widely used to induce and study damage.[3–7] In this letter we report experimental data showing that the energetic electron beam of a transmission electron microscope induces nucleation of damage at specific dislocation cores in a Si grain boundary. We also report atomistic simulations that provide an explanation for this effect and further predict a structural transformation that may occur under suitable experimental conditions.

The experimental study was performed on a silicon bicrystal wafer containing an isolated 16° symmetric tilt boundary with the tilt axis parallel to the $\langle 001\rangle$ direction ($\Sigma=25\{710\}\langle 001\rangle$). Plan view samples with a $\langle 001\rangle$ surface normal were prepared by mechanical polishing and ion milling with 1–3 keV Ar ions, which was followed by characterization with high resolution *Z*-contrast imaging using a HB603U scanning transmission electron microscope operating at 300 kV.

A symmetric $\Sigma=25$ boundary with a common $\{710\}$ plane can be constructed by rotating two crystalline regions about the $\langle 001\rangle$ axis through equal and opposite angles of 8.13°. The boundary structure is periodically repeated, with a period of one conventional lattice parameter ($a=5.43$ Å) parallel to the tilt axis, and a period of 38.4 Å ($a\sqrt{50}$) in a direction normal to the tilt axis. In each repeat period normal to the tilt axis the grain boundary consists of two extended cores, one being a mirror image of the other, separated by perfect crystalline regions. Figures 1(a) and 1(b) display, in the projection normal to the tilt axis, electron micrographs of one of these extended cores at two stages of exposure to electron irradiation: (a) a nearly unaffected core with appreciable intensity from all the columns; and (b) a partially affected core with a few of the columns having reduced brightness. Figure 2(a) displays in the same projection a three dimensional computer model of the boundary structure.

A closer look at the structure of Fig. 2(a) reveals that in the undamaged grain-boundary core there are four dislocation cores,[8] each dislocation core appearing as a ''pentagon-triangle'' combination in the projection normal to the tilt axis. All these cores have Burgers vectors in a plane normal to the tilt axis and are therefore designated perfect edge dislocations. Two of the cores, $D1$ and $D2$ are adjacent to each other and have opposite Burgers vectors, thereby constituting a dislocation dipole. The other two edge dislocation cores $E1$ and $E2$ have Burgers vectors $a/2\langle 110\rangle$ and $a/2\langle 1\bar{1}0\rangle$, respectively, where the x direction is taken normal to the boundary plane and the y direction taken in the grain boundary plane normal to the tilt axis. The Burgers vectors of $E1$ and $E2$ add up to a, which is the total dislocation content of the boundary core. We note that all the columns with reduced brightness in the damaged core are located on and around the edge dislocations $E1$ and $E2$. In the following, we discuss results of an extensive computational analysis to understand: (1) why a small region localized around $E1$ and

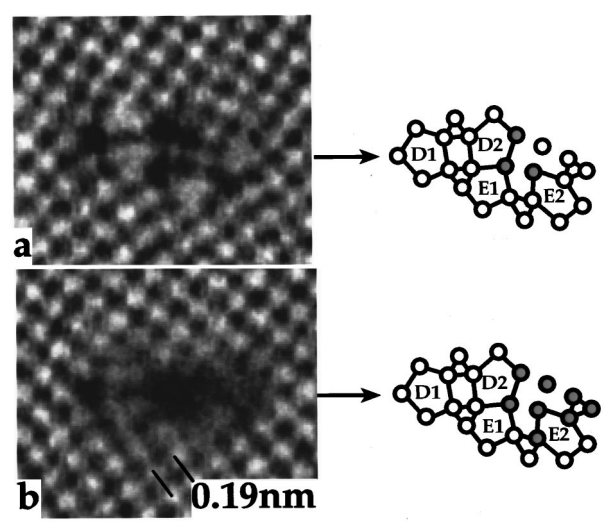

FIG. 1. *Z*-contrast images and derived structures of the $\Sigma=25$ $\{710\}$ $\langle 001\rangle$ symmetric tilt boundary at two stages of exposure to electron irradiation: (a) a nearly unaffected core with all columns visible but those shaded showing reduced intensity; (b) a partially affected core with several columns appearing darker.

[a]Present address: Molecular Simulations, Inc., Burlington, MA 01803.

 © 1999 American Institute of Physics
Downloaded 04 Jun 2004 to 160.91.48.238. Redistribution subject to AIP license or copyright, see http://apl.aip.org/apl/copyright.jsp

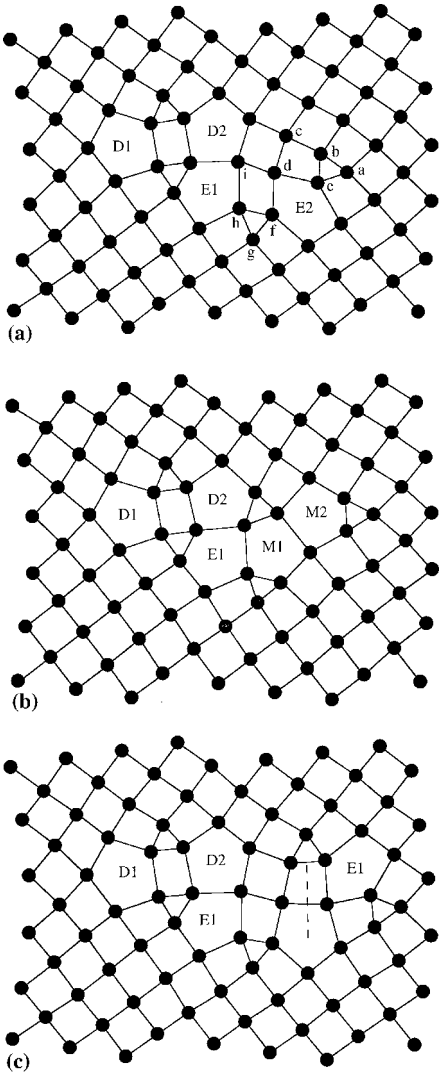

FIG. 2. (a) Three-dimensional atomic model of the boundary structure identifying the individual dislocations cores and labeling various sites. (b) The atomic structure of the transformed grain boundary resulting from the segregation of the [*b*,*c*] divacancy chain. The edge dislocation core $E2$ of the original grain boundary dissociates into two mixed dislocation cores $M1$ and $M2$. (c) The transformed structure resulting from the segregation of the [*a*,*b*] divacancy chain creating an extended edge dislocation core.

$E2$ is preferentially affected by electron irradiation, leaving the rest of the extended core unchanged; (2) the atomic scale processes that underlie the observed phenomenon; (3) any possible low-energy defect configuration that might lead to a structural transformation of the boundary.

In a relativistic elastic collision between an electron and an atomic nucleus initially at rest, the energy required to knock an atom out of its position and create structural damage, T_m must be greater than the ''displacement energy'' E_d. The displacement energy is somewhat larger than the formation energy of a Frenkel pair because of kinetic barriers and has been determined experimentally to be 15 ± 5 eV for a bulk Si crystal.[9,10] It is expected to be smaller at a grain boundary where the formation energy of a Frenkel pair is generally smaller (by 2–4 eV; see below). The fraction of atoms in a column initially knocked out by the electron beam (i.e., the fraction of Frenkel pair defects) is given by

$$f_F = n_{e1}\sigma_d. \tag{1}$$

Here, n_{e1} is the number of electrons passing through per unit area, estimated to be $\sim 10^5$ Å^2 from the scan time and the electron current in the microscope probe; σ_d is the total Mott scattering cross-section of the electron[11] which decreases rapidly with increasing E_d. Since Si is a light element, the Mott cross-section can be accurately computed using the McKinley–Feshbach formula.[12] Using appropriate values of E_d, we find that the electron beam creates 2%–5% vacancies in bulk atomic columns and as many as 20% in grain boundary columns. Point defects in Si are, however, known to be very mobile under electron irradiation conditions.[13] Therefore, these initial defects would either recombine, escape to the surface, or segregate at low-energy sites in the grain boundary. This analysis suggests that the low-intensity columns in Fig. 1(b) correspond to sites with large segregation energies of certain point defects.

To address the nature of these defects, we have computed the formation energies of both vacancies and interstitials in the bulk crystal and at various sites within the grain boundary core. The segregation energy is the difference between formation energies in the grain boundary and the bulk crystal. To describe the interatomic interaction for Si we used the many-body potential due to Tersoff,[14] which reproduces well the local density approximation (LDA) results for vacancy and interstitial formation energies in the bulk crystal (see Table III of Ref. 14 for more details). We tested the potential further against LDA results for vacancies at various sites in the $\Sigma=5\{310\}\langle 001\rangle$ tilt boundary, which has a smaller repeat cell than the $\Sigma=25$ boundary. Agreement was satisfactory for both formation energies and atomic relaxations.

For the $\Sigma=25$ boundary, we computed the formation energy of isolated vacancies, isolated divacancies, chains of monovacancies (i.e., removal of an entire column of atoms) and pairs, triplets, etc., of such chains. In each case, the relevant atom(s) were removed and the surrounding lattice fully relaxed using a combined scheme of simulated annealing and conjugate gradients. Similar calculations were done for self-interstitials.

Table I lists the formation energies (normalized per vacancy) of the most stable vacancy structures in various configurations. Figure 2(a) displays the site designations. The vacancy formation energies at other sites are at least 2.5 eV or higher. It is clear from the table that all the low-energy structures occur in a localized region of the core in and around the dark region in the micrograph of Fig. 1(b). From a similar computational study on the interstitials, we find that the lowest formation energies are around 2.5 eV, and the low-energy sites are scattered all over the dislocation core, showing no particular affinity to the low-intensity region of Fig. 1(b). These results lead to the conclusion that interstitials are not trapped in specific regions and either recombine with vacancies or move to the surface. We conclude that vacancies segregated in various low-energy configurations are primarily responsible for the low-intensity columns observed in Fig. 1(b).

A closer look at Table I shows that the chain configurations have lower formation energy than the isolated vacancies, which indicates a significant attraction between neighboring vacancies. However, of the many different chain configurations explored, two divacancy chain structures, i.e.,

Downloaded 04 Jun 2004 to 160.91.48.238. Redistribution subject to AIP license or copyright, see http://apl.aip.org/apl/copyright.jsp

TABLE I. The formation energies of the most stable vacancies in various configurations. Configurations are isolated unless indicated explicitly as a chain configuration. The letters indicate sites at which the vacancies are initially placed, as designated in Fig. 2(a).

Vacancy configurations	Formation energy (eV/vacancy)
bulk	3.7
[*b*]	1.7
[*d*]	1.7
[*i*]	1.8
[*a*,*b*]	1.0
[*b*,*c*]	1.6
[*b*] chain	0.8
[*d*] chain	1.4
[*d*,*i*] chain	1.3
[*a*,*b*] chain	0.3[a]
[*b*,*c*] chain	0.2[a]
[*a*,*b*,*e*] chain	1.2
[*f*,*g*,*h*] chain	1.4
[*b*,*c*,*d*,*e*] chain	1.3
[*d*,*f*,*h*,*i*] chain	1.3

[a]Structural transformation.

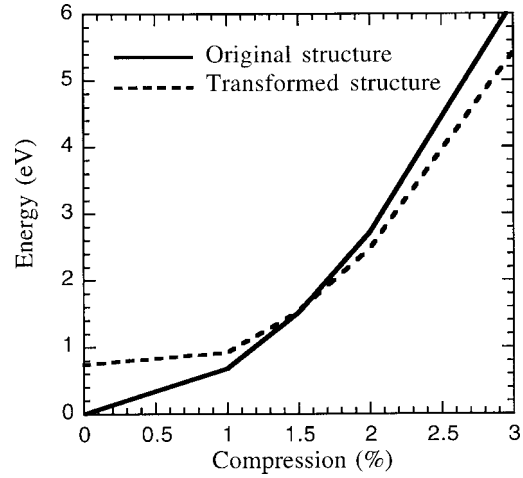

FIG. 3. A plot of the change in energy as a function of uniaxial compression perpendicular to the boundary plane of the original boundary of Fig. 2(a) and the transformed grain boundary of Fig. 2(b). Values are normalized per periodic segment of the grain boundary and are relative to the energy of the original boundary structure. A stability crossover occurs at a compression of ~1.5%.

the [*a*,*b*] chain and the [*b*,*c*] chain have extremely low formation energies, an order of magnitude smaller than the vacancy formation energy in the bulk.[15] Figures 2(b) and 2(c) display the structures following the relaxation of the [*b*,*c*] and the [*a*,*b*] divacancy chains, respectively. Both these structures have a noteworthy feature: all atoms are fourfold coordinated, i.e., the segregation of a chain of divacancies has led to a new structure without any dangling bonds!

A comparison of the dislocation cores of Figs. 2(a) and 2(b) indicates that the pure edge dislocation core $E2$ with Burger's vector $\mathbf{b}=a/2\langle 1\bar{1}0\rangle$ has dissociated into two mixed dislocations $M1(\mathbf{b_1}=a/2\langle 10\bar{1}\rangle)$ and $M2(\mathbf{b_2}=a/2\langle 0\bar{1}1\rangle)$, while all the other cores remain unchanged. The atomic arrangement shown in Fig. 2(c) is more complicated—here $E2$ splits up into an edge dislocation with Burger's vector $\mathbf{b}=a/2\langle \bar{1}10\rangle$ and an ''extended'' edge dislocation with $\mathbf{b}=a\langle 010\rangle$ indicated by the dotted line. These reconstructed dislocation cores have lower atomic density. In addition, we found that the formation energy of interstitials in these cores is reduced by almost an electron volt compared to that in the untransformed grain boundary, making them effective diffusion pipes. Another interesting feature is the presence of a chain of ''long'' bonds ~2.6 Å, which provide ideal sites for the cooperative segregation of certain dopants in the form of substitutional dimers.[16]

All the foregoing calculations were carried out under zero external stress. Figure 3 plots the change in energy as a function of uniaxial compression normal to the grain boundary plane for the original grain boundary [Fig. 2(a)] and the transformed grain boundary of Fig. 2(b). There is a stability crossover at a compression of ~1.5%. A large local compressive stress can thus drive the formation energy of the [*b*,*c*] divacancy chains negative and bring about a spontaneous structural transformation of the boundary. Such compression is commonly achieved in strained layer epitaxy.

As is evident from the micrographs of Fig. 1, electron irradiation can induce vacancy segregation in the select regions of the grain boundary core, but does not lead to the predicted reconstruction. The key difference is that the simulations involved annealing at high temperatures whereas the experiment was done at room temperature. Further experiments with different conditions would be needed to explore the relevant phase space, e.g., irradiation at elevated temperatures and/or pressures, which is not currently feasible on our instrument. Finally, external stress might be used to induce a spontaneous transformation.

We would like to thank Mark Robinson for useful discussions. This research was supported in part by Lockheed Martin Energy Research Corp. under DOE Contract No. DE-AC05-96OR22464, and ONR Grant No. N00014-96-1-1286, and by an appointment to the ORNL Postdoctoral Research Associates Program administered jointly by ORNL and ORISE.

[1] See, e.g., *Ion Implantation and Beam Processing*, edited by J. S. Williams and J. M. Poate (Academic, New York, 1984).
[2] G. J. Clark, A. D. Marwick, F. LeGoues, R. B. Laibowitz, R. Koch, and P. Madakson, Nucl. Instrum. Methods Phys. Res. B **32**, 405 (1988).
[3] L. W. Hobbs, Ultramicroscopy **3**, 381 (1978); A. Howie, Rev. Phys. Appl. **15**, 291 (1980).
[4] D. A. Muller and J. Silcox, Philos. Mag. A **71**, 1375 (1995).
[5] L. M. Wang, Nucl. Instrum. Methods Phys. Res. B **141**, 312 (1998).
[6] M. Kiritani, Ultramicroscopy **39**, 135 (1991).
[7] L. Reimer, Ultramicroscopy **14**, 291 (1984).
[8] We refer to these ''structural units'' as dislocations because they retain the characteristic ''edge,'' ''screw,'' or ''mixed'' character that isolated dislocations in bulk crystals exhibit. They are also characterized by Burger's vectors. This practice goes back to the classic paper by Hornstra [J. Hornstra, Physica **26**, 198 (1959)].
[9] L. Reimer, *Transmission Electron Microscopy* (Springer, New York, 1993), Chap. 5.
[10] J. W. Corbett and J. C. Bourgoin, in *Point Defects in Solids*, edited by J. H. Crawford and L. M. Slifkin (Plenum, New York, 1975), Vol. 2, Chap. 1, Sec. 7.
[11] N. F. Mott, Proc. R. Soc. London, Ser. A **135**, 429 (1932).
[12] W. A. McKinley and H. Feshbach, Phys. Rev. **74**, 1759 (1948).
[13] G. D. Watkins, in *Radiation Damage in Semiconductors* (Dunod, Paris, 1964), p. 97.
[14] J. Tersoff, Phys. Rev. B **38**, 9902 (1988).
[15] Chains of interstitials were also found to be more stable than isolated interstitials. However, the formation energy of the most stable chain was found to be around 0.9 eV per interstitial, significantly higher than the formation energy of the most stable divacancy chains.
[16] A. Maiti, M. F. Chisholm, S. J. Pennycook, and S. T. Pantelides, Phys. Rev. Lett. **77**, 1306 (1996).

Downloaded 04 Jun 2004 to 160.91.48.238. Redistribution subject to AIP license or copyright, see http://apl.aip.org/apl/copyright.jsp